*Article*

# An antibiofilm vector based on a modified β-cyclodextrin: Complexation study and biological activity.

**Jinan Abdelkader[1*], Magbool Alelyani[2,3], Yazeed Alashban[4], Sami A. Alghamdi[4], Youssef Bakkour[2, 3*]**

[1] Laboratory of Applied Chemistry (LAC), Department of chemistry, Faculty of Sciences III, Lebanese University, Campus Michel Sleiman, Ras Maska, Lebanon.
[2] Department of Radiological Sciences, College of Applied Medical Science, King Khalid University, Abha 61421, Saudi Arabia
[3] Central Research Laboratories (CRL), Laboratory of NMR, King Khalid University, Abha 61421, Saudi Arabia
[4] Radiological Sciences Department, College of Applied Medical Sciences, King Saud University, P.O. Box 145111, Riyadh 4545, Saudi Arabia.
* Correspondence: jinan.abdelkader@ul.edu.lb ; ybakkour@kku.edu.sa

**Abstract:** To face the high tolerance of biofilms to antibiotics, it is urgent to develop new strategies to fight against these bacterial consortia. We describe here an innovative antibiofilm nano vector, consisting of a Dispersin B-permethylated-β-cyclodextrin/ciprofloxacin adamantly (DspB-β-CD/CIP-Ad). For this purpose, complexation assays between CIP-Ad and (i) unmodified β-CD and (ii) different derivatives of β-CD, that are 2,3-O-dimethyl-β-CD, 2,6-O-dimethyl-β-CD, and 2,3,6-O-trimethyl-β-CD were tested. A stoichiometry of 1/1 was obtained for the β -CD/CIP-Ad complex by NMR analysis. ITC experiments were carried out to determine Ka, ΔH, ΔS thermodynamic parameters of the complex between β-CD or its different derivatives in the presence of CIP-Ad. A stoichiometry 1/1 of β-CD/CIP-Ad complexes was confirmed with variable affinity according to the type of methylation. A phase solubility study showed increased CIP-Ad solubility with CDs concentration, pointing out complex formation. The evaluation of the antibacterial activity of CIP-Ad and the 2,3-O-dimethyl-β-CD/CIP-Ad or 2,3,6-O-trimethyl-β-CD/CIP-Ad complexes was performed on *S.epidermidis* strains. MIC studies showed that the complex of CIP-Ad and 2,3-O-dimethyl-β-CD exhibited similar antimicrobial activity to CIP-Ad alone, while the interaction with 2,3,6-O-trimethyl-β-CD increased MIC values. Antimicrobial assays on *S. epidermidis* biofilms demonstrated that the synergistic effect observed with the DspB/CIP association was partly maintained with the 2,3-O-dimethyl-β-CDs/CIP-Ad complex. To obtain this "all in one" nano vector, able to destroy the biofilm matrix and release the antibiotic simultaneously, we covalently grafted DspB on three carboxylic permethylated CD derivatives with different length spacer arms. The strategy was validated by demonstrating that a DspB-permethylated-β-CD/ciprofloxacin-Ad nanovector exhibited efficient antibiofilm activity.

**Keywords:** Cyclodextrin; Ciprofloxacin; Dispersin B; Inclusion complex; Antibiofilm

## 1. Introduction

Staphylococcus epidermidis is a major infective agent in compromised patients, such as drug abusers or immunocompromised patients (for example, patients under immunosuppressive therapy, chronic wound patients, AIDS patients, and premature newborns). The ability to adhere and subsequently form biofilms on indwelling devices is among the potential virulence factors associated with S. epidermidis species [1][2][3]. Indeed, sessile organisms exhibit a high resistance to antimicrobials compared to their planktonic counterparts [4]. The Extracellular Polymeric Substances (EPS) of the biofilm matrix form the scaffold for a three-dimensional architecture, being involved in

 doi:10.20944/preprints202305.0022.v1



bacterial adhesion and biofilm cohesion [5]. EPS matrix also contributes to bacterial resistance against nonspecific and specific host defenses and antimicrobial agents [6][7][8][9][10][11][12]. Polysaccharides are a major fraction of this EPS matrix [5][13]. Most of them are linear or branched long molecules. Some of these polysaccharides are homopolysaccharides, including sucrose-derived glucans and fructans [13], but most of them are heteropolysaccharides that consist of a mixture of neutral and charged sugar residues. They can contain organic or inorganic substitutions that significantly affect their physical and biological properties.

Polycationic exopolysaccharides also exist, such as intercellular adhesin, which is composed of β-1,6-linked N-acetylglucosamine with partly deacetylated residues. The matrix-mediated antibiotic resistance is mainly due to a low metabolic activity and oxygen limitation within the biofilm [14]. The role of reduced antibiotic penetration in the drug resistance of biofilms, is highly antibiotic dependent, beta-lactams and vancomycin diffusion being significantly reduced, whereas the diffusion of aminosides and fluoroquinolones seems un-affected [14][15][16]. Some efficient Strategies for biofilms eradication are combinations of bacteria killing and matrix removal by using Detachment Promoting Agents (DPAs). Many of these DPAs were described in the literature, including enzymes and chemical agents [17]. They include in particular chelating agents, for example, EGTA [18], EDTA, NaCl, $CaCl_2$, or $MgCl_2$ [17]. Among agents having a promising clinical future, are biofilm-matrix degrading enzymes. Indeed, numerous studies pointed out the ability of these enzymes to inhibit the biofilm proliferation, detach preformed biofilms, and sensitize biofilms toward antimicrobials by depolymerizing either polysaccharides [19][20] or extracellular DNA [21]. DispersinB® (DspB) [22] was discovered in 2003 from Actinobacillus actinomycetemcomitans. Treatment of S. epidermidis biofilms with DspB caused dissolution of the EPS matrix and detachment of biofilm cells from the surface [20][23], and disrupted biofilm formation by Escherichia coli, S. epidermidis, Yersina pestis and Pseudomonas fluorescens [19]. One of the main drawbacks of the enzyme-based anti-biofilm strategy is that dispersal of bacteria from the biofilm may favor bloodstream infections, septic thrombophlebitis, endocarditis, metastatic Infections, and sepsis [2][24][25][26][27]. It is the reason why, most of the time, it is simultaneously or sequentially used in combination with antimicrobial agents.

Several studies also showed that DspB sensitizes biofilm bacteria to antibiotics [28][29][30], and macrophages [31]. A preliminary experiment, here performed, confirmed that DspB enhanced the activity of the ciprofloxacin (CIP) fluoroquinolone against biofilms when used simultaneously.

Synthetic fluoroquinolones and derivatives are broad-spectrum antibiotics that are widely used for the treatment of serious bacterial infections for human and veterinary use [32][33]. The structure-activity relationship of fluoroquinolones has been extensively investigated, and depends on the presence of the carboxyl, carbonyl and fluorine groups at $C_3$, $C_4$ and $C_6$ positions, respectively [34]. Moreover, the antibacterial effectiveness is highly improving if an amino substituent is present at $C_5$, an alkylated pyrrolidine or piperazine at $C_7$, a halogen at $C_8$, and a cyclopropyl group at N1 [34]. An interesting approach is the development of new quinolone-based antibacterial agents by chemical modification on the carboxylic acid for the preparation of quinolone-macrocycle conjugates [35]. Ciprofloxacin is one of the most commonly used fluoroquinolone in clinical field with for examples treatment of respiratory infections [36][37], meningitis [36], septicemia [36], intraabdominal infections [38], So, we designed a new antibiofilm vector, consisting to a DspB-β-cyclodextrin (β-CD)/CIP-Ad complex, combining both enzyme and antibiotic delivery. This vehicle is an “all-in-one” tool, which provides the ability to simultaneously destroy the biofilm matrix and release the antibiotic to achieve a combined effect (Figure 1).

 doi:10.20944/preprints202305.0022.v1



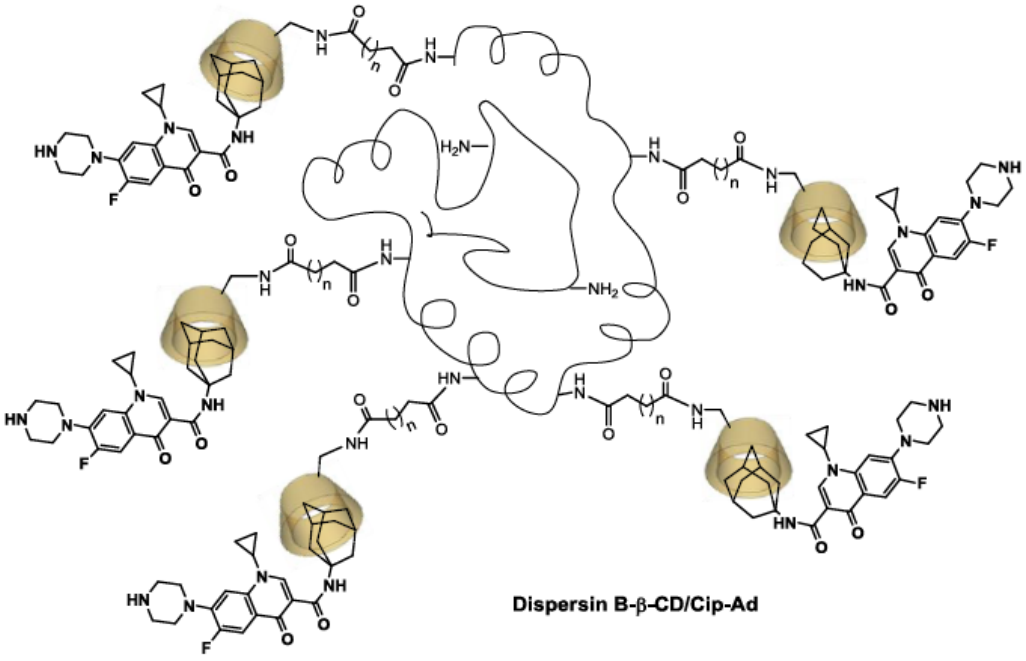


**Figure 1.** Nanovector based on a DspB-β-CD/CIP-Ad complex combining both antibiotic and biofilm dispersal enzyme.

β-CDs are truncated cone-shaped molecules composed of seven α(1-4)-glucose units. The 7 primary alcohols functions at C-6 position and the 14 secondary alcohols at the C-2 and C-3 positions constitute the primary and secondary faces of the macrocycle, respectively. This conformation forms a hydrophobic central cavity suitable for the inclusion of various organic molecules and a hydrophilic external surface. The main characteristic of CDs is the ability to insert the hydrophobic part of a guest molecule into the cavity. The formation of this host-guest inclusion complex and its stability also depend of the size and functionalization of the molecule [39].

Supramolecular chemistry of CDs has often been used in enzyme technology [40] with, as illustration, works of Villalonga et al. [41][42][43][44][45]. The authors demonstrated that immobilization of CD on surface of enzymes improved its affinity for the substrate and its thermostability while maintaining a good activity.

In order to overcome the impediment due to this weak interaction between the guest antibiotic and the host CD molecules, we synthesized an adamantyl ciprofloxacin derivative (CIP-Ad. Indeed, the high affinity of adamantyl group for the internal cavity of the macrocycle [46] will im prove the stability of the inclusion complex with the ciprofloxacin. Moreover, such supramolecular interaction should enhance the antibiotic solubility, stability, and bioavailability [47][48]. To develop this new concept, we firstly had to form an inclusion complex between the modified antibiotic (CIP-Ad) and various β-CDs, by preserving the antimicrobial activity.

Complexation of the CIP-Ad with native β-CD I and three methylated β-CD derivatives commercially-available, i.e., 2,3-O-dimethyl-β-CD II, 2,6-O-dimethyl-β-CD III, 2,3,6-O-trimethyl-β-CD IV (Figure 2), was thus performed, and investigated using isothermal titration calorimetry (ITC), in order to evaluate thermodynamic parameters of the interactions. The stoichiometry of the obtained complexes was determined using two dimensions Nuclear Overhauser Effect Spectroscopy (NOESY). The antibiofilm efficacy of DspB-CIP and DspB (2,3-O-dimethyl-β-CDs/CIP-Ad) complex was then tested on a mature Staphylococcus epidermidis biofilm model. To reach the one shot strategy, CDs were grafted on DspB via a covalent coupling strategy. In this context, we synthesized three carboxylic permethylated CDs derivatives with different spacer arms lengths at the C-6 position of

the CDs I, II and III (Figure 2). The antibiofilm activity of DspB-CDs conjugates was then investigated to evaluate the influence of such modification on the biofilm matrix.

Finally, we have validated our approach by demonstrating that DspB-2,3,6-O-trimethyl-β-CD/CIP-Ad nanovector exhibits an efficient antibiofilm activity.

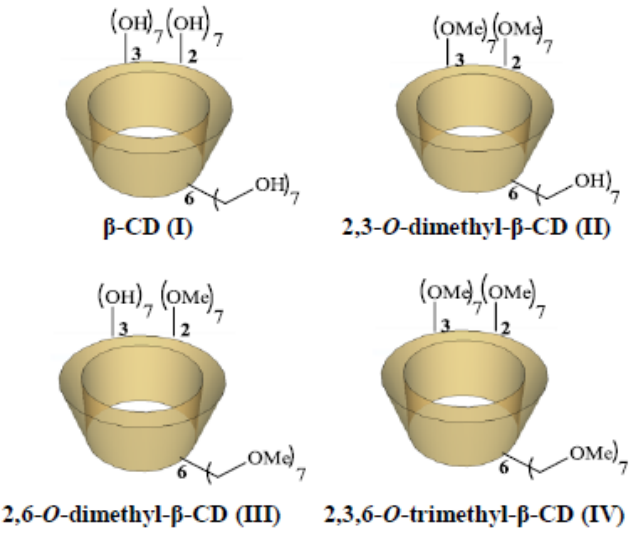


7

**Figure 2.** Schematic structure of β-CD (I), 2,3-O-dimethyl-β-CD (II), 2,6-O-dimethyl-β-CD (III), and 2,3,6-O-trimethyl-β-CD (IV).

## 2. Results

The use of an adamantyl group was chosen as molecular anchor to enhance the intermolecular interactions between the enzyme-conjugated CD and the antibiotic [46]. Furthermore, it was shown that adamantaplatensimycin (bioactive analogous of platensimycin) conserves an antibacterial activity against methicillin-resistant Staphylococcus aureus and vancomycin-resistant Enterococcus faecium [49]. The synthesis of CIP-Ad 4 derivative was obtained in three steps

(Scheme 1). After quantitative amino protection step, an efficient peptide coupling reagent was used in order to overcome the low reactivity of C-3 carboxylic acid of quinolone core. After deprotection step, the desired CIP-Ad 4 was obtained quantitatively.

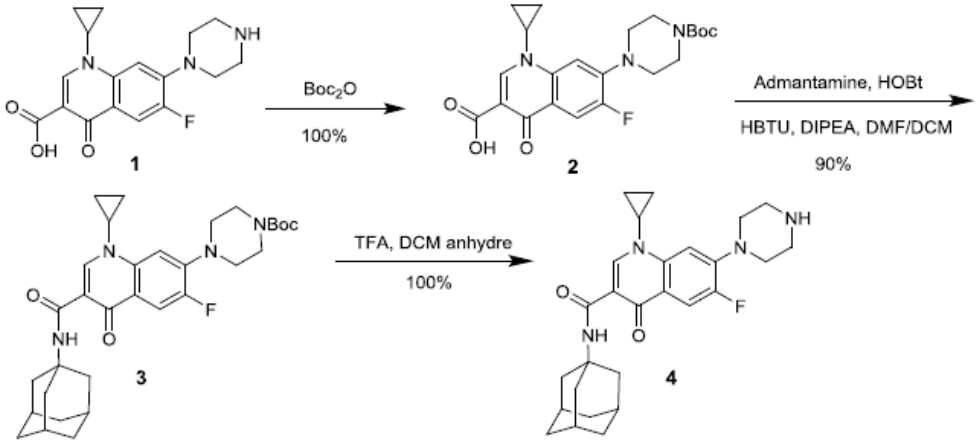


**Scheme 1.** Synthesis of ciprofloxacin derivative 4 (CIP-Ad) bearing adamantyl group at C-3 position.

### *2.1. NMR Study*

 doi:10.20944/preprints202305.0022.v1



The aim of the NMR study was to highlight and describe the inclusion properties and factors affecting the complexation between CIP-Ad 4 with β-CD I. In the structure of β-CDs, $H_3$ and $H_5$ protons are located inside the cavity, whereas $H_2$ and $H_4$ are outside the torus (Figure 3). The H6 protons of the primary alcohol group are on the narrow side, and the $H_1$ are in the glycosidic bond plane of β-CD. Therefore, the formation of inclusion complexes is usually highlighted, in the proton NMR spectrum, by the shift and the deformation of $H_3$ and $H_5$ NMR signals.

So an assignment of $^1$H NMR spectra of the free forms of CIP-Ad 4, β-CD I and the β-CD I/CIPAd 4 complex in D2O/DCl at pH=3 (Figure 3) was achieved by 2D NMR 1H/1H COSY (Figure 1S) as well as $^1$H/$^1$H NOESY (Figure 2S) and the chemical shifts are summarized in Table 1. As expected, β-CD's $H_3$, $H_5$ protons signals were the most affected by the inclusion as their signals were significantly broaden and shifted by Δδ=0.02 ppm and 0.01 ppm respectively. Regarding the CIP-Ad 4 part, the chemical shifts of adamantyl protons $H_{11}$, $H_{11'}$, $H_{12}$ and the aromatic protons $H_2$, $H_5$ and $H_8$ were modified by the inclusion.

**Table 1.** 1H NMR chemical shifts (ppm) of free β-CD I, free CIP-Ad 4 and β-CD I/CIP-Ad 4 complex (D2O/DCl, pH=3, 298K).

| **β-CD protons** | **$H_1$** | | **$H_2$** | **$H_3$** | **$H_4$** | **$H_5$, $H_6$** | |
|---|---|---|---|---|---|---|---|
| **Free β-CD (*)** | **5.02** | | **3.60** | 3.91 | 3.53 | 3.82 | |
| β-CD/CIP-Ad Complex | 5.02 | | 3.60 | 3.89 | 3.54 | 3.81 | |
| Δδ (free-complex) | 0.00 | | 0.00 | 0.02 | -0.01 | 0.01 | |
| **CIP-Ad protons** | **$H_{1a}$,H1b** | **$H_{1c}$** | **$H_2$** | **$H_5$** | **$H_{7a}$,$H_{7b}$** | **$H_8$** | **$H_{11}$,$H_{11'}$** | **$H_{12}$** |
| Free CIP-Ad | 1.35; 1.08 | 3.60 | 8.60 | 7.62 | 3.55; 3.47 | 7.49 | 2.01, 1.67 | 2.04 |
| β-CD/ CIP-Ad Complex | 1.38; 1.10 | 3.75 | 8.6 | 7.93 | *3.57*; 3.47 | 7.67 | 2.15, 1.78 | 2.25 |
| Δδ (free-complex) | 0.03; 0.02 | -0.15 | 0.06 | -0.31 | *(0.02)*; 0.00 | -0.18 | -0.14,-0.11 | -0.21 |

(*) δHi obtained for β-CD were consistent with those published in literature [50][51]. The values in italics are ambiguous due to the superposition of peaks.

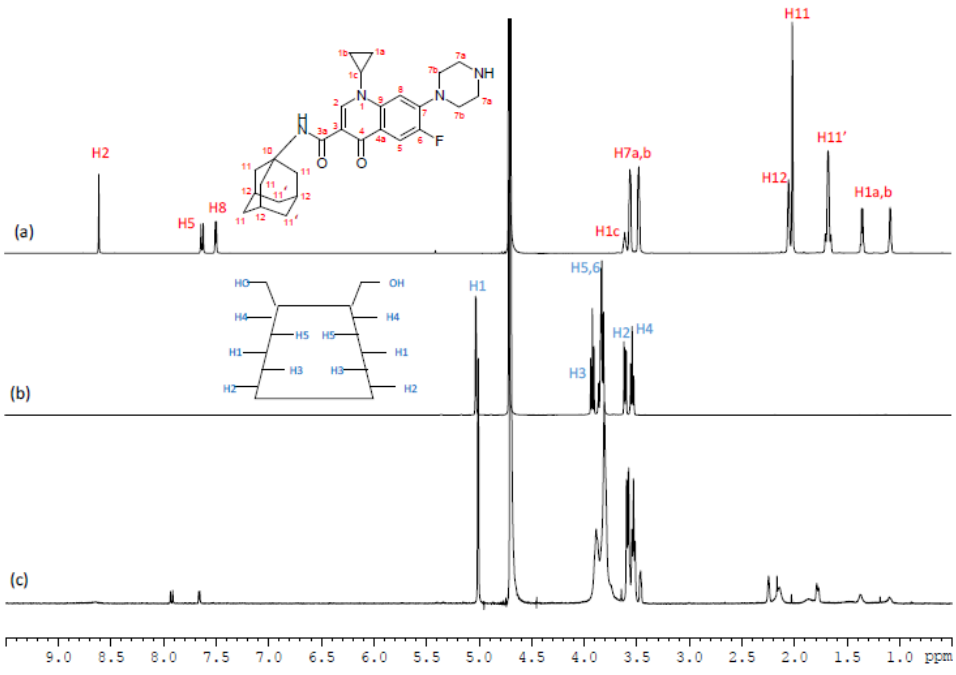


**Figure 3.** $^1$H NMR spectra (D2O/DCl, pH=3, 298 K, 600 MHz) of free CIP-Ad 4 (a), free β-CD I (b) and the β-CD I/CIP-Ad 4 complex (c).

The classic method of Job's Plot, usually used to determine the stoichiometry of this type of complex, was not effective in our case, because of the very low solubility of the CIP-Ad **4** molecule. Nevertheless, from the structural information obtained from the 2D $^{1}H/^{1}H$ NOESY spectrum of the complex, it was possible to determine the orientation of the CIP-Ad **4** molecule in the cavity of the β–CD and to indirectly deduce the stoichiometry of the β-CD **I**/CIP-Ad **4** complex. The 2D $^{1}H/^{1}H$ NOESY spectrum of the β-CD **I**/CIP-Ad **4** complex (Figure 4) exhibited cross peaks between the adamantyl protons (H11, H11', H12) of CIP-Ad **4** and protons H3 and H5 of β-CD **I** confirming the inclusion of adamantyl group of CIP-Ad **4** in the β-CD cavity. On the contrary, the absence of correlation between H3, H5 of β-CD **I** and H7a, H7b of CIP-Ad **4**, suggested no inclusion of the piperazinyl group.

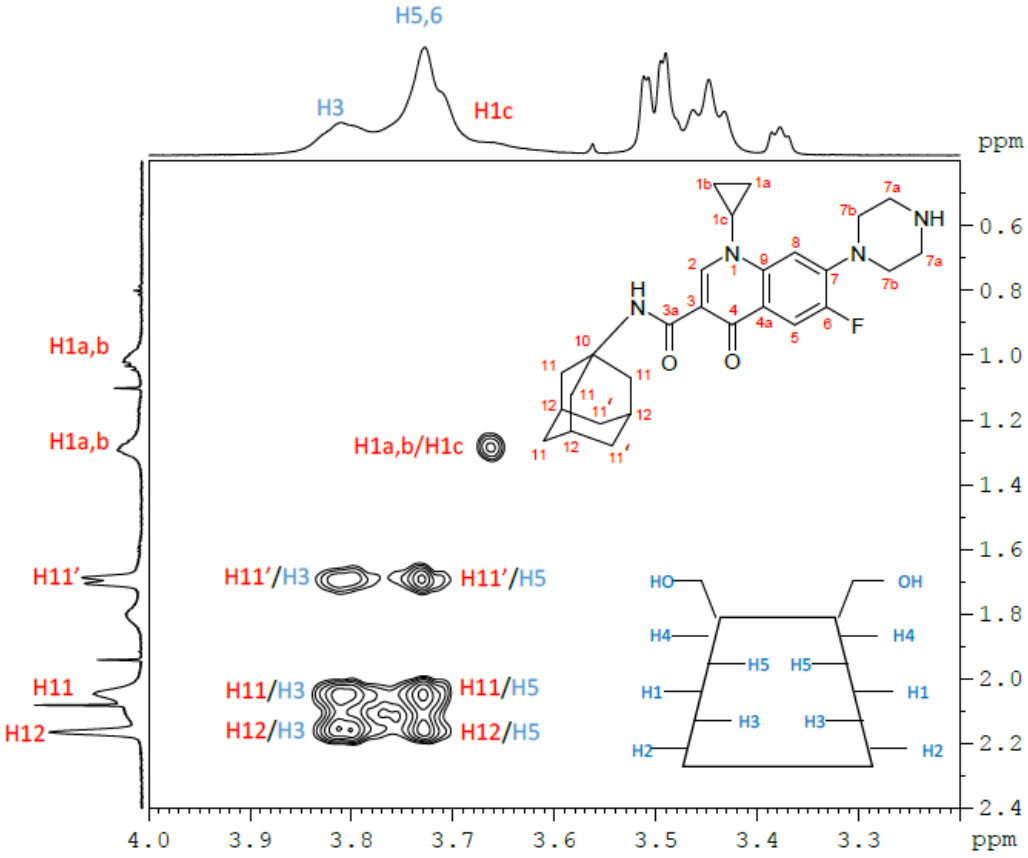


**Figure 4.** Magnification of the 2D $^{1}H/^{1}H$ NOESY NMR spectrum ($D_2O$/DCl, pH=3, 290 K, 600. MHz) of the β-CD I/CIP-Ad 4 complex. The cross peaks assignment appears directly on the map, in blue for β-CD protons and in red for CIP-Ad protons.

These results were in favor of a β-CD I/CIP-Ad 4 complex with a 1/1 stoichiometry by the adamantyl side of CIP-Ad **4** (Figure 5).

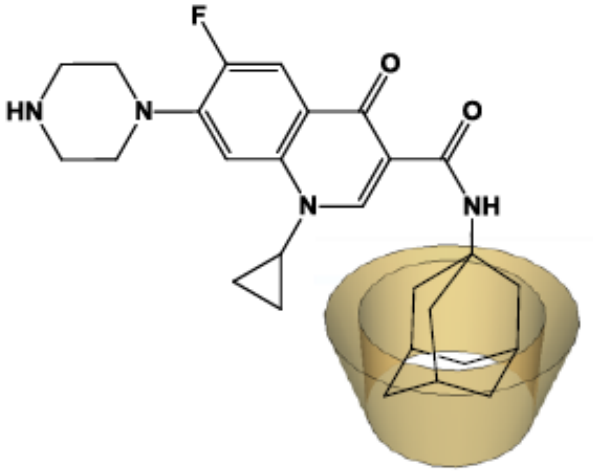


**Figure 5.** The β-CD I/CIP-Ad 4 1/1 inclusion complex in $D_2O$/DCl at pH=3.

*2.2. ITC studies*

ITC experiments were then carried out for the determination of thermodynamic parameters (Ka, ΔH, ΔS) and stoichiometries of CIP-Ad and β-CD I, 2,3-*O*-dimethyl-β-CD II, 2,6-*O*-dimethyl-β- CD III and, 2,3,6-*O*-trimethyl-β-CD IV complexes (Figure 2). Experiments were performed in acidic medium, leading to the protonated form of CIP-Ad 4. The heat generated during the association process was provided in μJ/mol of titrant (host, I, II, III, IV), in the respect of titrant / titrate molar fraction (host, I, II, III, IV / guest CIP-Ad). The experimental titration curve was fitted through a one-site-independent binding model [52]. The value of the apparent binding stoichiometry (n) was extracted by the inflection point of the curve. As all the curves were perfectly sigmoid, an accurate determination of n was obtained.

The thermodynamics parameters were determined at different temperatures (15-60°C) for all β-CDs (I, II, III, IV) hosts. The experimental titration curves of CIP-Ad 4 by β-CD I at 25°C showed an equivalence point for approximately 1/1 molar ratio of β-CD/CIP-Ad, confirming the observed NMR data. Same stoichiometry was obtained for all host molecules (II, III, IV). The fitting of the binding curves gave direct measurement of affinity constant Ka and enthalpy variation ΔH, then, thanks to thermodynamic equations, Gibbs free energy ΔG and entropy variation ΔS (Table 3) were determined [52]. Variation of heat capacity ΔCp values was calculated as the slope of the curve correlated to the enthalpy values versus the temperature.

**Table 3.** Thermodynamic parameters for the complexation of ciprofloxacin derivative (CIP-Ad 4) with hosts I, II, III, IV. Thermodynamics parameters were obtained using a one-site-independent binding model of NanoAnalyse software (interaction of "n" ligands with macromolecule with one binding site). C corresponds to the Wiseman's parameter.

| Host | T (°C) | Ka/$10^4$ ($M^{-1}$) | ΔH (kJ/mol) | ΔS (J/mol.K) | ΔG (kJ/mol) | ΔCp (J/mol.K) | C |
|---|---|---|---|---|---|---|---|
| β-CD I | 15 | 44.5 ± 4.6 | -17.8 ± 0.1 | 46.2 | -31.1 | -201 ($r^2$= 0.996) | 134 |
| | 25 | 33.5 ± 3.2 | -19.9 ± 0.1 | 38.9 | -31.5 | | 101 |
| | 37 | 21.3 ± 1.4 | -21.9 ± 0.1 | 31.4 | -31.6 | | 64 |
| | 45 | 17.9 ± 1,3 | -23.8 ± 0.2 | 25.7 | -31.9 | | 54 |
| | 55 | 15.1 ± 1.1 | -25.7 ± 0.2 | 20.8 | -32.5 | | 45 |
| | 60 | 10.7 ± 0.7 | -27.1 ± 0.2 | 15.1 | -32.0 | | 32 |
| 2,3-*O*-dimethyl-β-CD II | 25 | 1.1 ± 0.1 | -5.7 ± 0.1 | 58.5 | -23.1 | -320 ($r^2$= 0.962) | 3 |
| | 37 | 1.0 ± 0.1 | -10.1 ± 0.3 | 43.8 | -23.7 | | 3 |
| | 45 | 0.9 ± 0.2 | -13.7 ± 0.6 | 32.5 | -24.1 | | 3 |
| | 55 | 0.8 ± 0.1 | -16.5 ± 0.6 | 23.8 | -24.6 | | 2 |
| | 60 | 0.7 ± 0.1 | -16.3 ± 0.6 | 24.6 | -24.5 | | 2 |

| | | | | | | | |
|---|---|---|---|---|---|---|---|
| 2,6-*O*-dimethyl-β-CD III | 15 | 114.0 ± 22.0 | -9.9 ± 0.1 | 81.7 | -33.3 | -438 ($r^2$= 0.989) | 342 |
| | 25 | 94.5 ± 5.5 | -13.3 ± 0.1 | 69.8 | -34.0 | | 284 |
| | 37 | 72.7 ± 6.7 | -18.6 ± 0.1 | 52.3 | -34.7 | | 218 |
| | 45 | 60.1 ± 3.6 | -21.0 ± 0.1 | 44.7 | -35.1 | | 180 |
| | 55 | 39.9 ± 2.7 | -27.4 ± 0.4 | 23.7 | -35.1 | | 120 |
| | 60 | 37.5 ± 3.2 | -29.4 ± 0.2 | 18.4 | -35.5 | | 113 |
| 2,3,6-*O*-trimethyl-β-CD IV | 15 | 13.4 ± 1.5 | -11.3 ± 0.1- | 58.7 | -28.2 | -537 ($r^2$= 0.982) | 40 |
| | 25 | 12.1 ± 1.3 | -19.6 ± 0.2 | 31.4 | -29.0 | | 36 |
| | 37 | 8.4 ± 0.7 | -22.7 ± 0.2 | 21.2 | -29.2 | | 25 |
| | 45 | 6.5 ± 0.4 | -28.3 ± 0.2 | 3.2 | -29.3 | | 20 |
| | 55 | 4.6 ± 0.3 | -34.7 ± 0.4 | -16.6 | -29.2 | | 14 |
| | 60 | 3.6 ± 0.2 | -35.8 ± 0.4 | -20.2 | -29.0 | | 11 |

Usually, to validate the ITC experiments, Wiseman's "C" parameter [53] has to be between 10 and 500-1000 [53][54]. In the present study, all C values are in the optimal experimental window, excepted for II / CIP-Ad complex (C value around 2-3) (Table 3). However, Turnbull and Daranas demonstrated that even for low affinity system with weak C value from 0.01 to 10 (Ka =$10^2$ $M^{-1}$), the ITC results are still valide [55]. In this case, three conditions have to be respected: *i*) a use a sufficient portion of the binding isotherm for analysis; *ii*) a precise knowledge of the binding stoichiometry n and of the concentrations of ligand and receptor; *iii*) an adequate ratio of signal to noise. These criteria are filled for the present study with CIP-Ad/β-CD II complex. The host-guest inclusion complex represents the distribution of species in equilibrium giving an average stoichiometry and a binding constant Ka [39][52]. In the present study, this equilibrium constant Ka was calculated for CIP-Ad/β-CD I complex around $10^5$ $M^{-1}$ at 37°C (i.e., ΔG ≈ -30 kJ/mol). This strong association constant is due to perfect fitting of adamantyl moiety inside the β-CD cavity. Consequently, the presence of large CIP structure bound to adamantyl group produced no change in the inclusion process, as reported in the literature with other adamantane derivatives (ΔG° ≈ -20 to -30 kJ / mol) [56][57]. Different values of association constant were obtained for methylated β-CDs (II, III and IV) ranging from $10^4$ to $10^6$ $M^{-1}$ at 37°C (i.e., ΔG from -23 to -35 kJ/mol). The highest binding constant was observed with the CIP-Ad/β-CD III (Ka = 72.7 $10^4$ $M^{-1}$), followed by the CIP-Ad/β-CD I (Ka = 21.3 $10^4$ $M^{-1}$), the CIP-Ad/β-CD IV (Ka = 8.4 $10^4$ $M^{-1}$), and CIP-Ad/β-CD II (Ka = 1.0 $10^4$ $M^{-1}$) complexes. The binding strength is clearly dependent on the host molecule functionalization. Such differences have been already reported in the literature with adamantyl derivatives in favor of β-CD [56][57]. We observed a spontaneaous complexation (ΔG<0) for all CIP-Ad/β-CDs complexes (I to IV) with thermodynamically favorable enthalpy and entropy values (ΔH<0 and ΔS>0). Complexations of CIP-Ad with I and IV are enthalpy-driven (|ΔH|>|TΔS|) on all the temperature range studied, while interactions with II and III are entropy-driven (|ΔH|<|TΔS|) for lower temperatures before becoming enthalpy-driven for higher temperatures. A negative ΔCp was obtained for all CIP-Ad/β-CDs complexes (I to IV). The possible driving forces involved in the formation of inclusion complex with CDs are numerous, such as Van der Waals, hydrophobic, electrostatic, and hydrogen bonding, as well as charge–transfer interactions [39][58]. Moreover, others additional constraints, such as release of conformational strain and exclusion of cavity-bound high energy water, can be implicated [39][58]. In literature, a simple evaluation of enthalpy and entropy changes is usually used to distinguish dominance of hydrophobic or Van der Waals forces during complexation; hydrophobic interactions leading to ΔH>0 and ΔS>0 and Van der Waals interactions to ΔH<0 and ΔS<0. In fact, interpretation of thermodynamic parameters is more complex. One reason is that the formation of an inclusion complex is often accompanied by the release of water molecules from the CD cavity, which are at higher level of energy in comparison with those in external medium. This highly-energetic exclusion phenomenon also contributes to the negative enthalpy and entropy changes observed [58]. Others authors traditionally admit that complexation is governed by hydrophobic interactions when the process is entropy-driven, with larger and positive entropy and smaller enthalpy (|ΔH|<|TΔS| with ΔS>0). As opposed, usually Van der Waals interactions would be enthalpy-driven processes with minor favorable or unfavorable entropies interaction (|ΔH|>|TΔS| with ΔS>0 or ΔS<0). Consequently, hydrophobic and Vander Waals interactions would be the two principal forces leading to the

complexation for CIPAd/β-CDs (I to IV) complexes. However, study on a large temperature range permitted to access ΔCp and to discriminate the major force. When a negative ΔCp is obtained, hydrophobic bounds are formed as sequence of breakdown water clathrates around apolar molecules corroborating the desolvatation hypothesis of β-CD [58]. In contrast, hydrogen bond between β-CD and the guest makes a positive contribution to ΔCp [59]. Consequently, the large negative ΔCp values observed here for CIP-Ad/β-CDs complexes, confirmed the contribution of hydrophobic interactions as main driving forces.

*2.3. Solubility studies*

CIP-Ad **4** solubility was measured in water to evaluate its behavior near to physiological pH. Phase-solubility profiles are given in Figure 6A and 6B for native CD I and derivated II, III, IV, respectively. CIP-Ad is a poorly soluble drug with an intrinsic solubility ($S_0$) in water determined around $1.10^{-6}$ M. The solubility of CIP-Ad significantly increased in function of the CD concentration. According Higuchi and Connors classification [60], the solubility curves can be considered as A$_L$-type, that is a linear increase in solubility of CIP-Ad versus CD concentration is obtained. When 1/1 complexation is supposed between drug and CD, a linear correlation is attempted between the total solubility of drug ($S_t$) and the total concentration of cyclodextrin ($[CD]_t$) in the aqueous medium (equation 1):

$$S_t = S_0 + \frac{K_{1/1} S_0}{1 + K_{1/1} S_0} [CD]t$$

where $S_0$ is the intrinsic solubility of CIP-Ad (i.e. the solubility when non CD is present) and $K_{1/1}$ the apparent stability constant of the drug/CD complex. The plot of St versus $[CD]_t$ gives a straight line with a slope $K_{1/1} S_0 / (1 + K_{1/1} S_0)$) less than unity and an intercept ($S_{int}$) equal to $S_0$. Next $K_{1/1}$ can be determined from the slope and $S_0$ according the equation 2:

$$K_{1/1} = \frac{\text{Slope}}{S_0 (1 - \text{slope})}$$ Eq 2 according to Loftsson et al. [61]

Linear fit with a slope less than unity was obtained for all CDs, in the range of CD concentration studied, confirming the 1/1 stoichiometry of interaction. However, $S_{int}$ values were far from $S_0$ for all CDs and a negative value was obtained for host CD IV. This negative deviation from linearity at low CD concentration (i.e. $S_{int} < S_o$), reported as A$_L$-type phase-solubility profile in literature, is currently observed for poorly soluble drugs ($S_0 < 1.10^{-4}$ M) [61]. It could be due to the nonideality of water as a solvent, the self-association of the drug molecules and of the drug/CD complexes, as well as non-inclusion complexation phenomena [61]. The use of incorrect $S_{int}$ values results in an overestimation of K (or even negative K in the case of negative $S_{int}$) [61]. Consequently, the determination of K was here made from experimental value of $S_0$. K values around $66.10^4$ $M^{-1}$, $6.10^4$ $M^{-1}$, $52.10^4$ $M^{-1}$ and $37.10^4$ $M^{-1}$ were obtained for I, II, III and IV host molecules respectively. In comparison with ITC results, slightly higher values (excepted for III) were obtained, which could be attributed to the more hydrophobic form of CIP-Ad **4** in water than in acidic buffer (that is, the net charge of molecule is lower).

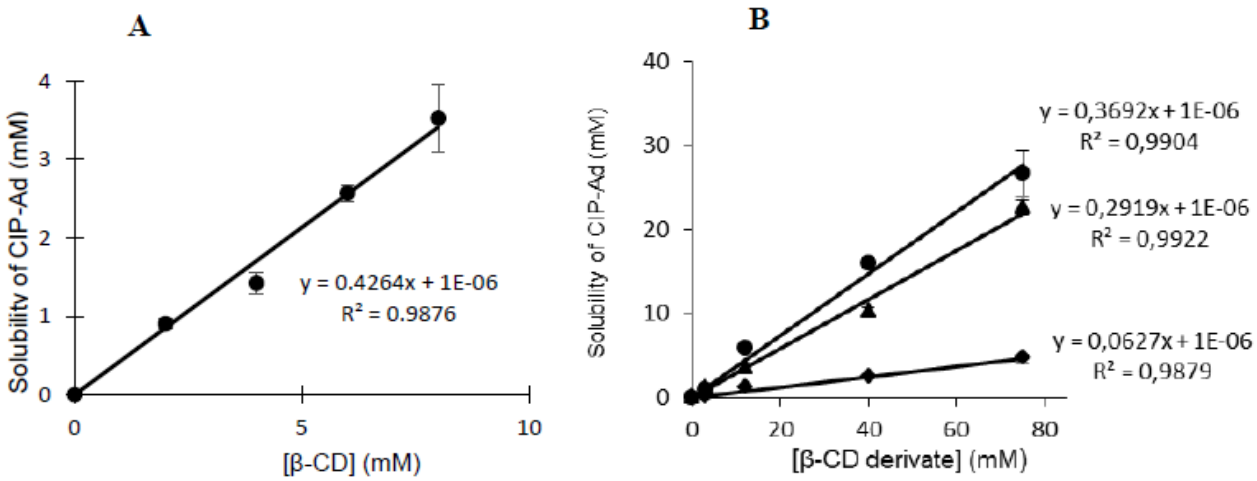


**Figure 6.** Evolution of the CIP-Ad **4** solubility according to the CD concentration: (A) natural β-CD I and (B) CD derivatives, ♦ (II), ● (III), ▲ (IV). An excess of CIP-Ad **4** was added to CD solutions. Bars: S.E (n = 3).

*2.4. Antimicrobial efficacy of Ciprofloxacin*

In order to thereafter evaluate the antimicrobial efficacy of CIP against *S. epidermidis*, Minimal Inhibitory Concentrations (MICs) values of the antibiotic were measured through the microdilution method based on ISO standard 20776 [62]. Experiments were performed in microplates, filled with Tryptic Soy Broth (TSB), with an initial bacterial concentration of $10^6$ CFU/mL. Values ranging from 0.25 to 4 µg/mL were obtained for CIP depending on the tested strain (Table 4).

**Table 4.** MIC values of CIP measured for the four S. epidermidis strains.

| Strain | 5 | RP62A | 1457 | 9142 |
|---|---|---|---|---|
| MIC (µg/mL) | 0.25 | 0.50 | 0.50 | 4.00 |

Strain 5 was the most sensitive and was consequently used for most of the further investigations. It is well known that biofilms correspond to high cell-density systems. It is the reason why the efficacy of high CIP concentrations was tested against high cell- density planktonic cultures. Experiments were performed in 96-well microplates containing TSB inoculated with an initial bacterial concentration of about 109 CFU/ mL. Bacteria were enumerated by plating out on Tryptic Soy Agar medium after incubation for 24h at 37°C. Time-killing curves are given on Figure 7. The exposure of planktonic cells to 10 x MIC (i.e., 2.5 µg/mL) of antibiotic during 24 hours, allowed a reduction of 3 log of the bacterial population.

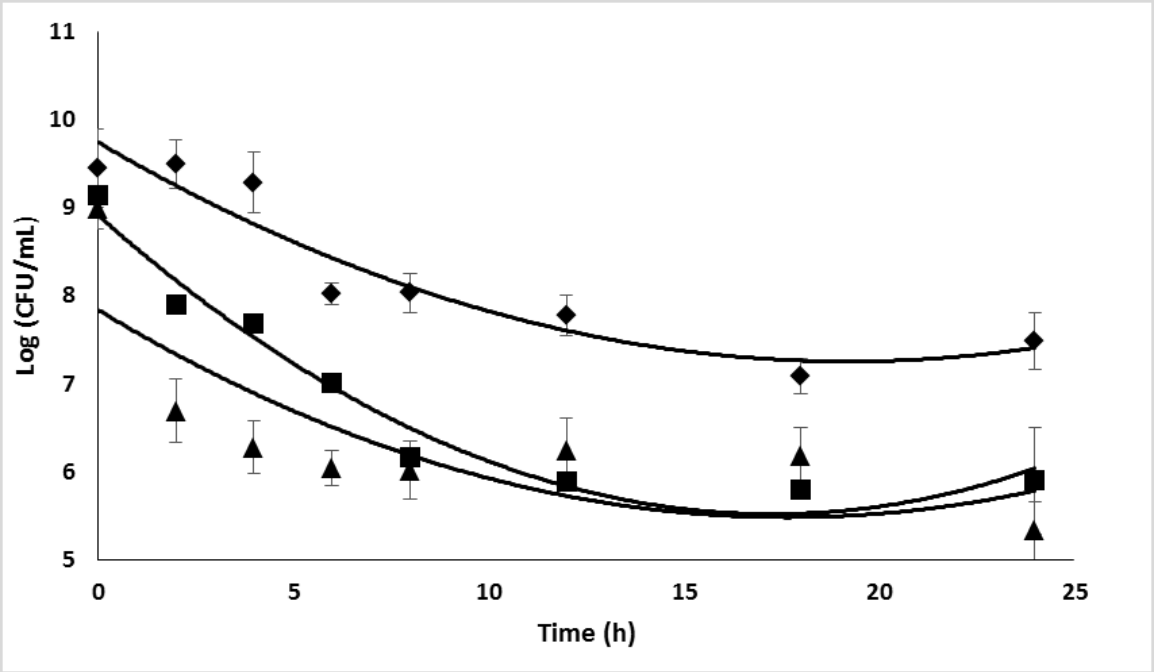


**Figure 7.** Efficacy of high CIP concentrations on high cell-density planktonic cultures of *S.epidermidis* (strain 5). ◆, 5 x MIC; ■, 10 x MIC; ▲, 20 x MIC. Bars: SE (n=3).

The increase of the antibiotic concentration to 20 x MIC did not significantly improve the treatment efficacy. For this reason, the highest tested CIP concentration was set to 2.5 µg/mL for further experiments.

Biofilms were formed in 96-well microplates containing 200 µl of TSB, as previously described [63]. The ability of *S. epidermidis* species to produce β-(1-6)-*N*-acetyl-D-glucosamine polymer (PNAG), results from the presence of the *ica* locus, which controls the production of the polysaccharide intercellular adhesin (PIA) [1]. The detailed structural elucidation of PNAG has been so far performed on different *S. epidermidis* [64][65]. Strain 5 was isolated from an infected orthopedic prosthesis [66]. Biofilms formed by this strain contained considerable amounts of PNAG as testified by very similar $^{1}$H NMR data that observed for the RP62A and 9142 strains [64][65].

The ability of strain 5 to form a biofilm was confirmed by measuring the sessile population in microplates after 24 hours of incubation. The results demonstrated that the strain was able to form a biofilm, the sessile population reaching about 1 x $10^{9}$ CFU/mL (SE n= 8). This bacterial concentration has been consequently used to test the different compounds on planktonic cells. The antimicrobial effect of CIP and DspB was then investigated on sessile microorganisms (strain 5). After 24h of incubation, wells were washed with Phosphate-Buffered Saline, and filled with 200 µL of TSB enriched with 5 µg/mL DspB and/or increasing amounts of CIP. After 2h of treatment at 37°C, the number of adherent bacteria before and after treatment was compared. Results given in Figure 8 confirmed the high resistance of sessile organisms to CIP since only 1 log kill was observed after exposure for 24 hours to a high antibiotic concentration (12.5 µg/mL, that is 50 x MIC).

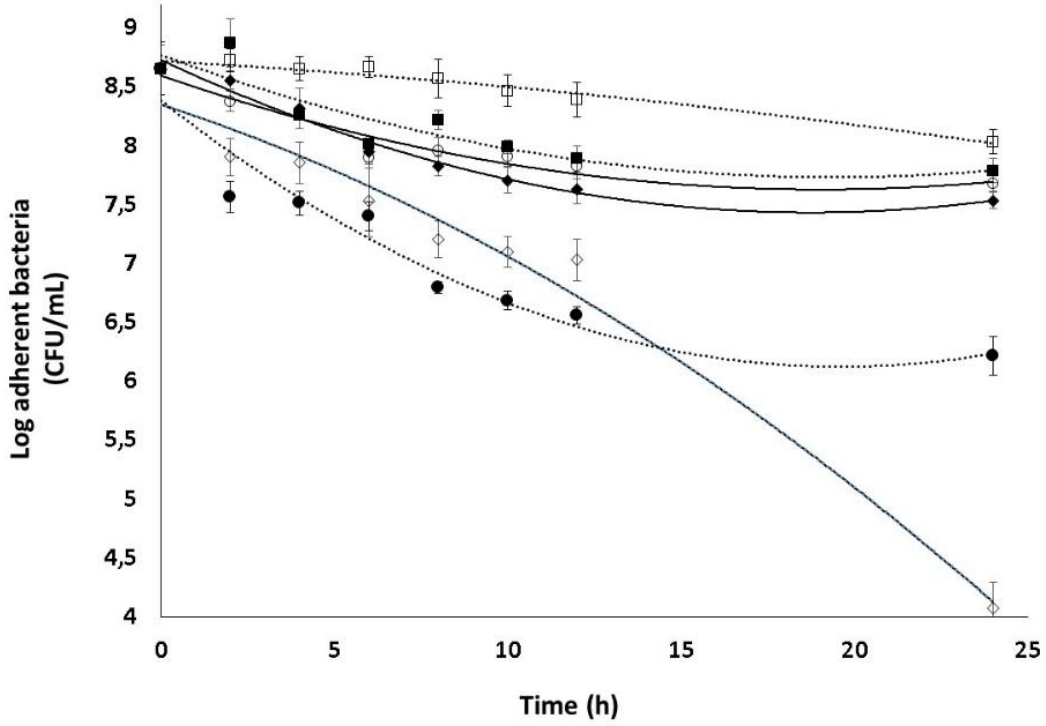


**Figure 8.** Susceptibility of *S. epidermidis* biofilm cells (strain 5) to: □, 5 µg/mL DspB; ■, 10 x MIC CIP; ○, 20 x MIC CIP; ♦, 50 x MIC CIP; ●, 100 x MIC CIP; ◊, 10 x MIC CIP and 5 µg/mL DspB, bars, SE (n=3).

DspB used alone as control, did not exhibit an antimicrobial activity. DspB and CIP exerted a synergistic effect against the biofilm, confirming bibliographic data [28][29][30]. Used together at the concentrations of 5 µg/mL DspB and 2.5 µg/ mL CIP (that is 10 x MIC), a bactericidal effect (5 log kill) was indeed observed on sessile organisms after exposure for 24 hours. This result showed that DspB increases the bacteria susceptibility to CIP. Finally, MICs of the CIP-Ad **4** were evaluated on the four *S. epidermidis* strains. The corresponding MICs are given in Table 5.

**Table 5.** MIC values of the CIP-Ad 4 on the four S. epidermidis strains.

| Strain | 5 | RP62A | 1457 | 9142 |
|---|---|---|---|---|
| MIC (µg / mL) | 2.0 | 4.0 | 4.0 | 8.0 |

Results points out that, for the four strains used, an antibacterial activity of the CIP-Ad **4** was observed, with higher MIC values than those measured for CIP, however (Table 4). Here again, strain 5 was the most sensitive strain.

*2.5. Combined effect of Dsp B and β-CD II/CIP-Ad complex against biofilms.*

The limited bibliographical data pertaining to the CIP interaction with CDs (e.g., dissolution, absorption) makes difficult the prediction of the drug delivery processes. Several mechanisms can contribute to drug release after parenteral administration [67][68], such as drug dilution, competitive displacement by endogenous materials, drug binding to plasma and tissue components, and drug uptake into non targeted tissues. The pharmacokinetic drug properties should be unaffected by the use of CDs, when binding constant is below $10^5$ $M^{-1}$ [69]. Consequently, two candidates appeared particularly suitable for further studies: the 2,3-*O*-dimethyl-β-CD (II)/CIP-Ad and the 2,3,6-*O*-trimethyl-β-CD (IV)/CIP-Ad complexes.

MICs of the two complexes against the 4 strains are given on Table 6. Results showed that complexation of CIP-Ad **4** with the 2,3-*O*-dimethyl-β-CD (II) did not alter the CIP-Ad derivative activity while complexation with the permethylated β-CD (IV) increased the MIC value on the four tested strains. For these reasons, the 2,3-*O*-dimethyl-β-CD (II)/CIP-Ad complex was used for further experiments. Again, strain 5 exhibited a higher susceptibility.

**Table 6.** MIC values of β-CD II/CIP-Ad complex and β-CD IV/CIP-Ad complex on the four *S.epidermidis* strains.

| Strain | Complex | |
|---|---|---|
| | **β-CD II/CIP-Ad** | **β-CD IV/CIP-Ad** |
| **5** | 2 | 4 |
| **RP62A** | 4 | 8 |
| **1457** | 4 | 8 |
| **9142** | 8 | 16 |

The susceptibility of planktonic bacteria against the β-CD II/CIP-Ad complex was then evaluated as described above. The concentrations used corresponded to 2.5 x and 10 x MIC CIP-Ad. Results (Figure 9) exhibited an expected increase in the antimicrobial activity as the complex concentration increased, the 24 hours exposure to the complex at 10 x MIC, leading to more than a 3log unit reduction of the bacterial population.

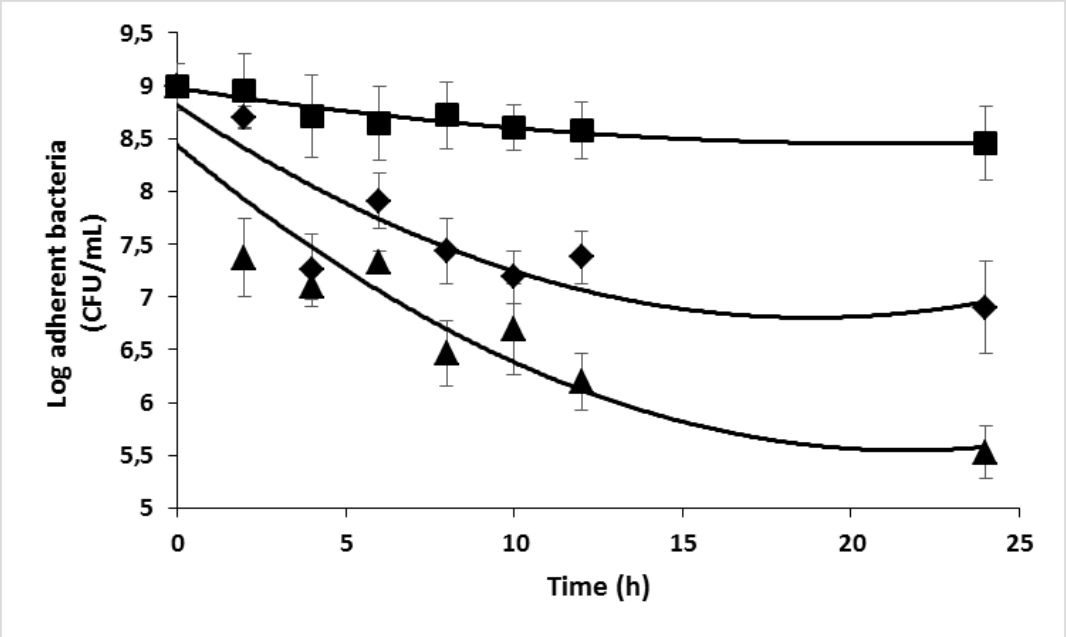


**Figure 9.** Susceptibility of planktonic *S. epidermidis* cells (strain 5) to II / CIP-Ad complex; ■, 2. MIC ♦, 5 MIC; ▲, 10 MIC; Bars, SE (n=3).

Before investigating the antimicrobial activity of the association DspB / β-CD II/CIP-Ad complex, on sessile organisms, the efficacy of the alone complex was evaluated (Figure 10).

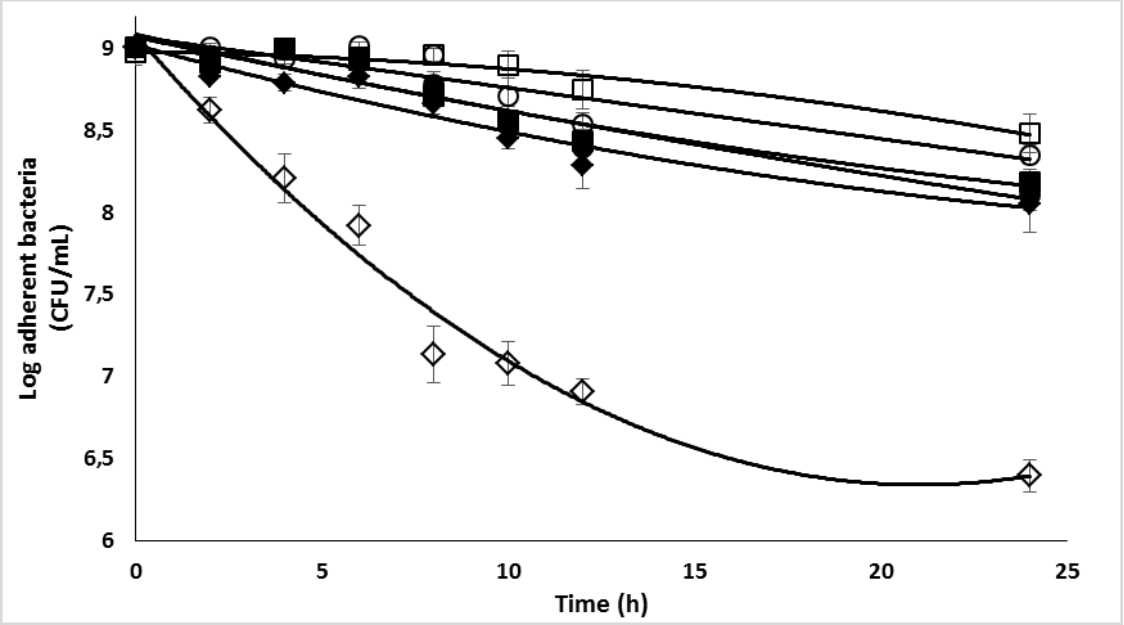


**Figure 10.** Antimicrobial activity of 2,3-*O*-dimethyl-β-CD II/CIP-Ad complex used alone or in association with DspB against *S. epidermidis* biofilms. □, control; DspB (5 µg/mL); ○, 5 x MIC; ■, 10 x MIC; ●, 20 x MIC; ♦, 50 x MIC; ◊, 5 x MIC and 5 µg /mL DspB.

Results showed that this complex exhibited the same activity against sessile organisms than the CIP (see Figure 8). For example, about 1 log unit decrease of the bacterial population was observed for 50 x MIC. When used in association with 5 µg/mL DspB, a reduction of 2 log unit of the sessile population was observed after 24 hours of exposure (Figure 10). These data confirmed the positive effect of the association, a control experiment confirming the absence of antimicrobial activity of DspB when used alone.

*2.6. Synthesis of CD derivatives CD1-3*

In order to elaborate DspB-β-CDs conjugates, we synthesized three carboxylic CDs derivatives with different spacer arm lengths, i.e., with 2, 4 and 10 atoms of carbon, named CD1, CD2 and CD3, respectively (Scheme 2). We focused this preliminary study on permethylated cyclodextrins, because easier to purify in large quantity. From this 6-*O*-monofunctionalization, the DspB was grafted via an amidation reaction (Scheme 3). The strategy used for the functionalization of the β-CD core involved the synthesis of the well-known mono-6-*O*-tosyl-β-CD precursor **5** [70]. After the introduction of the azide function, the macrocyle **6** was permethylated as described in the literature. A reduction step afforded the monoamino derivative **8** [70], ready for a coupling reaction with succinic anhydride [71], monomethyl adipic acid ester **a** or monomethyl dodecanedioic acid ester **b** at room temperature [45]. The corresponding 6-monoalkylcarboxyl-β-CDs derivatives, **CD1**, **CD2**, and **CD3,** were obtained after a saponification step.

 doi:10.20944/preprints202305.0022.v1



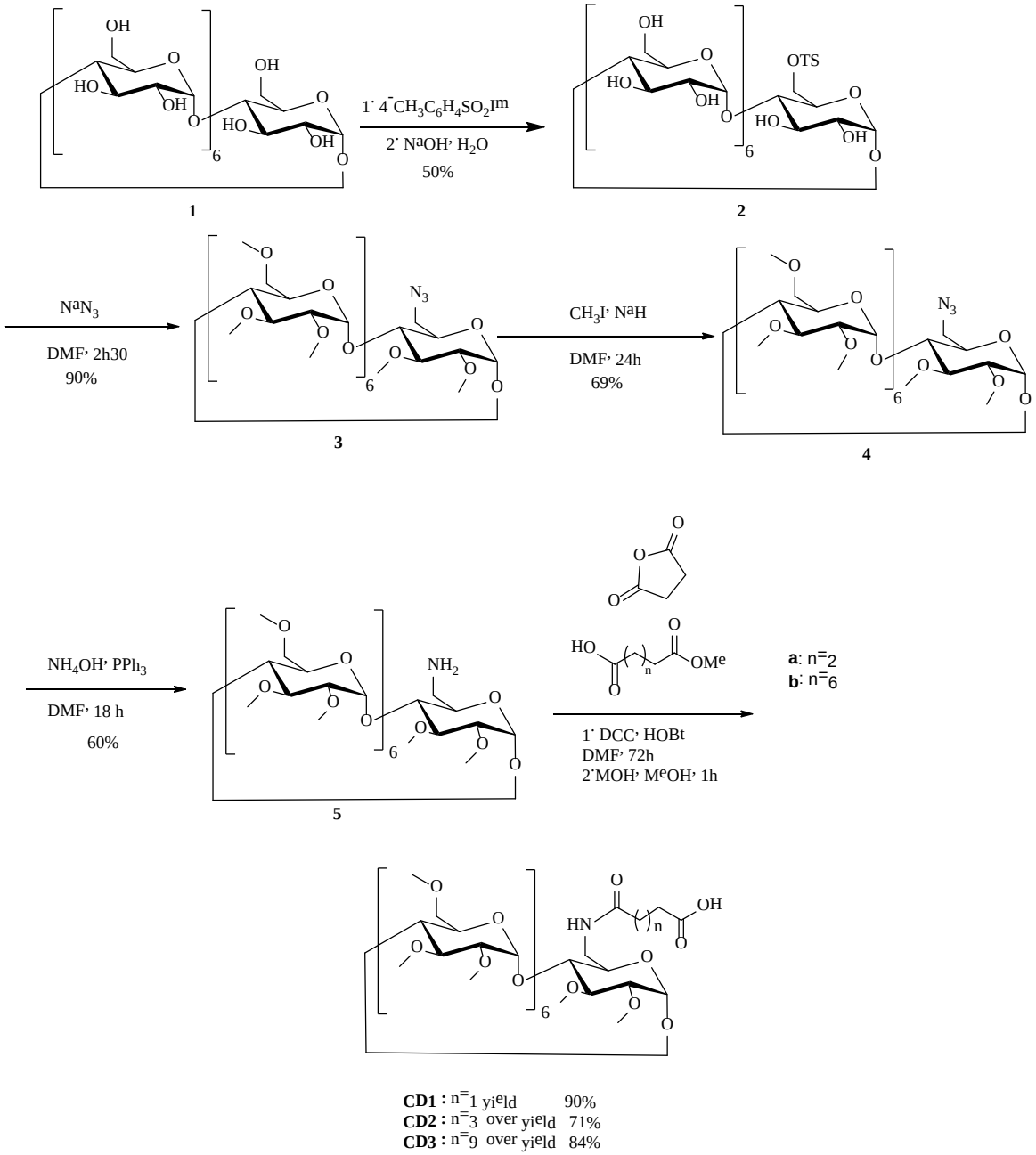


**Scheme 2.** Synthesis of the CD derivatives with different arm lengths, n=1 CD1; n=3 CD2; n=9. CD3.

The immobilization of the DispersinB® on the three macrocycles (CD1, CD2 and CD3) was performed with 1-ethyl-3-(3-dimethylaminopropyl)carbodiimide hydrochloride (EDAC) and *N*hydroxysuccinimide (NHS) in borate buffer (Scheme 3). After ultrafiltration of enzymatic solution, the modified DspB was purified using a 2-D Clean-Up Kit (GE Healthcare).

 doi:10.20944/preprints202305.0022.v1



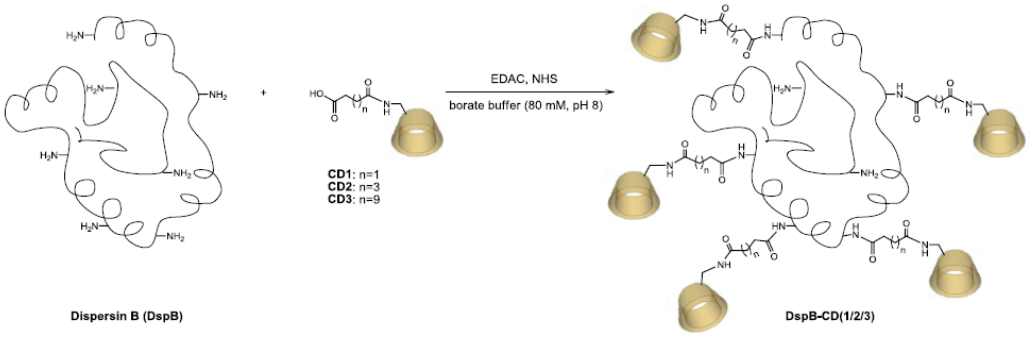


**Scheme 3.** Grafting of CD1/CD2/CD3 to DispersinB®.

Mass spectrometry analyses confirmed the expected masses of 69994; 48106 and 51171 g/mol for **CD1**, **CD2** and **CD3** with maximum rates of 17, 4 and 9 molecules per enzyme, respectively (data not shown). Native DspB was never found on MS spectra (data not shown), suggesting high grafting rate of DspB onto modified CDs.

*2.7. Enzymatic biofilm dispersion assays by DspB- β-CDs conjugates*

Tests were adapted from the method implemented by O'Toole and Kolter [72]. Briefly, bacteria were grown for 24 h in TSB at 37°C in microplates. Unattached cells were removed by rinsing the wells thoroughly with PBS, and biofilms were subsequently stained by incubation with Crystal Violet (CV). CV was then solubilized by adding ethanol and the OD of the solution measured at 550 nm.

The antibiofilm activity of the three DspB-β-CDs conjugates (that is bearing the 3 different arms) is given in Figure 11. Results showed that the conjugate bearing the shorter arm (CD1), exhibited the lower activity (highlighted by high OD values), whereas no alteration of the enzyme activity was observed with the two other conjugates (CD2 and CD3), as compared with DspB alone. As expected, this activity was concentration dependent. The enzymatic alteration observed with CD1 is probably due to a steric effect, the high number of CDs grafted onto the enzyme (17 per enzyme molecule) and the proximity of CDs restricting substrate accessibility to the active sites.

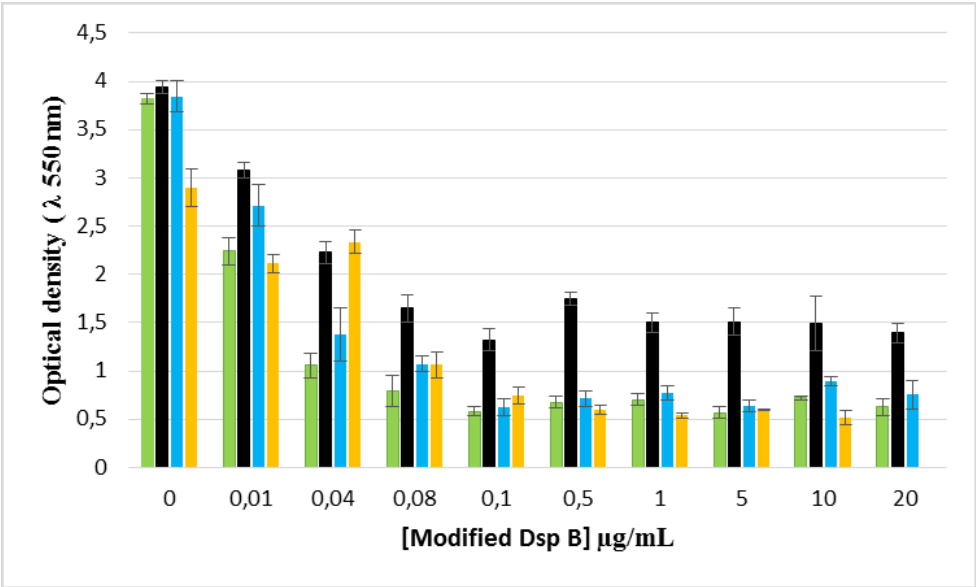


**Figure 11.** Effect of different concentrations of DspB-β-CDs conjugate on 24 hours-old biofilms (strain 5). Green bars, DspB; black bars, DspB-CD1; blue bars, DspB-CD2; yellow bars, DspBCD3 bars: SE (n=3).

 doi:10.20944/preprints202305.0022.v1



These results were then confirmed on the three other *S. epidermidis* strains (Figure 12). Results showed that the conjugate was efficient on all biofilms, confirming that the three strains produced PNAG. Here again, the DspB-CD1 conjugate exhibited the lowest antibiofilm activity.

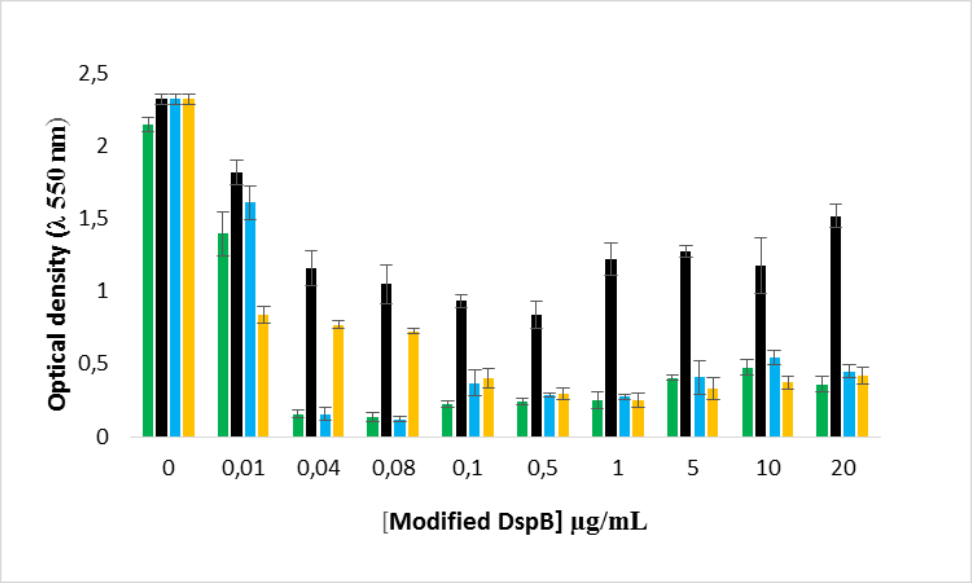


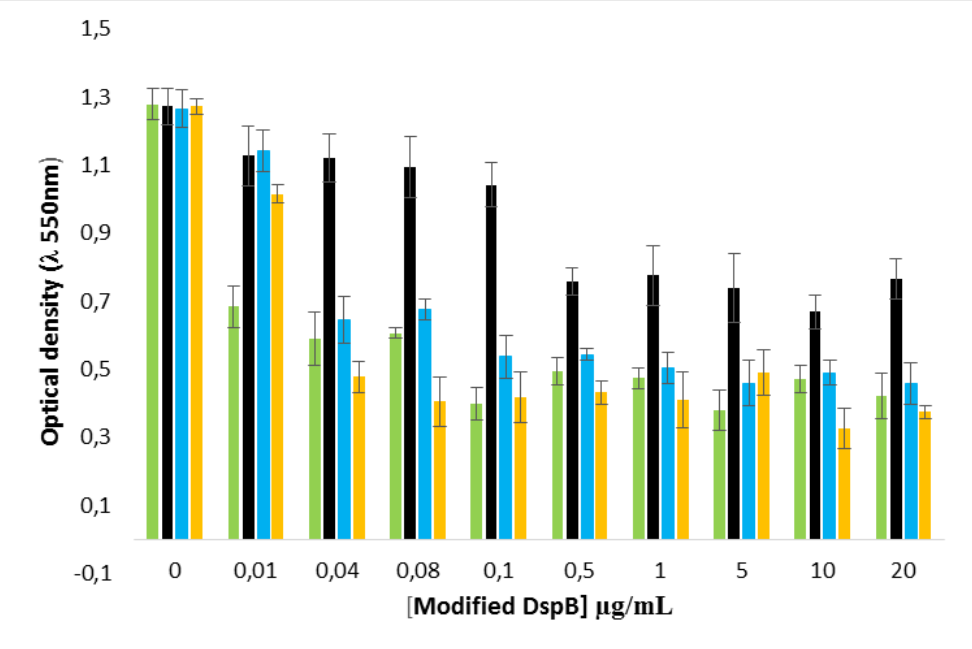

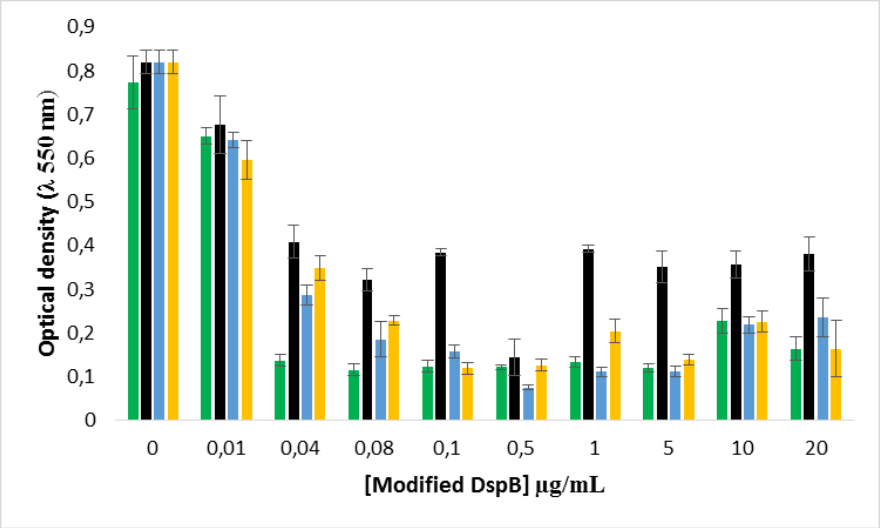


**Figure 12.** Comparison of the antibiofilm efficacy of DspB-β-CDs conjugate against 24h-old biofilms formed by strains RP62A, 1457 and 9142. A, strain RP62A; B, strain 1457; C; strain 9142. Green bars, DspB; black, DspB-CD1; bleu bars, DspB -CD2; yellow bars, DspB-CD3. Bars, S.E. (n+3).

*2.8. Effect of the DspB-β-CD3/CIP-Ad conjugate on biofilm of S. epidermidis*

Finally, we tested the antimicrobial activity of the nanovector DspB-β-CD3/CIP-Ad conjugate on strain 5 biofilms. A CIP concentration of 5 x MIC, i.e., 10 µg / mL was used. A significant activity of the vector was observed (Figure 13) on a 24 h-old biofilm, since about a 3 log reduction of the sessile bacterial population was observed after 24 hours of exposure. This activity was logically lower than that recorded with the association DspB/CIP (Figure 8) as a lower CIP concentration was used. The efficiency of the nanovector is similar to that obtained when the 2,3-*O*-dimethyl-β-CD (II)/CIP-Ad complex was used in association with the DspB (Figure 10) which demonstrates that chemical immobilization of CDs on DspB doesn't alter its antibiofilm properties.

## 3. Discussion

Complexation assays between adamantyl group grafted on ciprofloxacin, CIP-Ad, and four β-cyclodextrins derivatives, i.e, β-CD, 2,3-*O*-dimethyl-β-CD, 2,6-*O*-dimethyl-β-CD, and 2,3,6-*O*-trimethyl-β-CD, were investigated. A phase solubility study confirmed an increase of the CIP-Ad solubility with CD concentration, pointing out to a complex formation. NMR and ITC experiments showed a stoichiometry 1/1 of the β-CD/CIP-Ad complexes with an affinity depending on the type of methylation of β-CD. Due to their moderate affinity constant, 2,3-*O*-dimethyl-β-CD/CIP-Ad and permethylated-β-CDs/CIP-Ad complexes were selected for the antibacterial studies. The evaluation of the antibacterial activity of both CIP-Ad and β-CD derivatives/CIP-Ad complexes was performed on different *S. epidermidis* strains. MICs values showed that the 2,3-*O*-dimethyl-β-CDs did not alter the CIP-Ad activity, while complexation with permethylated-β-

CDs increased MIC values. Antibiofilm assays, then performed on *S. epidermidis* biofilms, confirmed the synergistic effect observed with the association of DspB/CIP which was partly maintained in presence of the complex formed between the modified antibiotic CIP-Ad and the 2,3-*O*dimethyl-β-CD. DspB was then modified with different CDs conjugates through chemical covalent coupling with carboxylic permethylated CDs derivatives with various spacer length. We showed that theses modified DspB with the CD conjugates maintained their antibiofilm activities. We validated our approach by demonstrating that the DspB-permethylated-β-CD/ciprofloxacin-Ad nanovector exhibited an efficient antibiofilm activity. Biofilm-associated infections are particularly problematic because sessile bacteria are able to withstand host immune defense response and are drastically more resistant to antimicrobials than their planktonic counterparts [4][73].

This is all the more true in the context of implanted medical device (for example, prosthesis or catheters), nocosomial, or depressed immune system related infections. Among the Staphylococcal species that appear in the list of leading etiologic agents, *S. epidermidis* is the second after *Staphylococcus aureus* [1][2][3][73], hence our choice. In the last decade, several innovative strategies have been published to fight against biofilms, some of them being patented. Among these strategies, modifications of surfaces to prevent adhesion and / or kill adherent bacteria have been proposed [74][75]. However, these approaches are not completely satisfactory due to their limited efficiency. Consequently, the main anti-infection tool used today in the medical field remains the antibiotherapy approach with often highly limited efficiency due to the high resistance of sessile bacteria to most antibiotics [4]. Faced with this assessment, anti-biofilm enzyme based approaches (as the nanovector presented here) constitute a promising alternative. Due to their ability to degrade the biofilm polymer matrix, they highly increase the efficiency of some antibiotics by both modifying the environmental conditions within the biofilm (for example, dissolved oxygen concentration levels) and by increasing drug diffusivity. Some of these enzymes are already marketed. Thus, the pulmozyme® (dornase alpha) a recombinant human deoxyribonuclease I (rhDNase), is inhaled to improve lung function in cystic fibrosis [76] and mechanically ventilated patients [77]. However, as already mentioned, the main drawback of this enzymatic antibiofilm strategy is the risk of live bacteria dispersal, hence the use of antibiotics in association. Though future investigations are required in order to improve the efficacy of the approach, the present concept presents the high advantage of being an "all-in-one" tool, and constitutes a real progress compared to conventional antibiotherapy treatments used by clinicians today.

**ACKNOWLEDGMENT:** The authors extend their appreciation to the Deanship of Scientific Research at King Khalid University for funding this work through large group Research Project under grant number RGP2/358/44.

**REFERENCES**

[1] D. McKenney, J. Hübner, E. Muller, Y. Wang, D.A. Goldmann, G.B. Pier, The ica locus of Staphylococcus epidermidis encodes production of the capsular polysaccharide/adhesin, Infect. Immun. 66 (1998) 4711–4720.

[2] M. Otto, Staphylococcal Infections: Mechanisms of Biofilm Maturation and Detachment as Critical Determinants of Pathogenicity, Annu. Rev. Med. 64 (2013) 175–188. doi:10.1146/annurev-med-042711-140023.

[3] C. Von Eiff, G. Peters, C. Heilmann, Pathogenesis of infections due to coagulase-negative staphylococci, Lancet Infect. Dis. 2 (2002) 677–685. doi:10.1016/S1473-3099(02)00438-3.

[4] J.W. Costerton, P.S. Stewart, E.P. Greenberg, Bacterial Biofilms: A Common Cause of Persistent Infections, Science (80-. ). 284 (1999) 1318–1322. doi:10.1126/science.284.5418.1318.

[5] H.-C. Flemming, J. Wingender, The biofilm matrix, Nat. Rev. Microbiol. 8 (2010) 623–633. doi:doi: 10.1038/nrmicro2415.

[6] C. Soumet, C. Ragimbeau, P. Maris, Screening of benzalkonium chloride resistance in Listeria monocytogenes strains isolated during cold smoked fish production, Lett. Appl. Microbiol. 41 (2005) 291–296. doi:10.1111/j.1472-765X.2005.01763.x.

[7] K. Ganeshnarayan, S.M. Shah, M.R. Libera, A. Santostefano, J.B. Kaplan, Poly-Nacetylglucosamine matrix polysaccharide impedes fluid convection and transport of the cationic surfactant cetylpyridinium chloride through bacterial biofilms, Appl. Environ. Microbiol. 75 (2009) 1308–1314. doi:10.1128/AEM.01900-08.

[8] H. Nakamura, K.-I. Takakura, Y. Sone, Y. Itano, Y. Nishikawa, Biofilm Formation and Resistance to Benzalkonium Chloride in Listeria monocytogenes Isolated from a Fish Processing Plant, J. Food Prot. 76 (2013) 1179–1186. doi:10.4315/0362-028X.JFP-12-225.

[9] E.A. Izano, M.A. Amarante, W.B. Kher, J.B. Kaplan, Differential roles of poly-Nacetylglucosamine

surface polysaccharide and extracellular DNA in Staphylococcus aureus and Staphylococcus epidermidis biofilms, Appl. Environ. Microbiol. 74 (2008) 470–476. doi:10.1128/AEM.02073-07.

[10] M. Otto, Staphylococcus epidermidis - The "accidental" pathogen, Nat. Rev. Microbiol. 7 (2009) 555–567. doi:10.1038/nrmicro2182.

[11] S. Jabbouri, I. Sadovskaya, Characteristics of the biofilm matrix and its role as a possible target for the detection and eradication of Staphylococcus epidermidis associated with medical implant infections, FEMS Immunol. Med. Microbiol. 60 (2010) 280–291. doi:10.1111/j.1574-695X.2010.00695.x.

[12] G. Rf, R. Gk, G.B. Kostiner, Time-kill efficacy of antibiotics in combination with rifampin against Staphylococcus epidermidis biofilms, Adv Perit Dial. 10 (1994) 189–92.

[13] P.M. Bales, E.M. Renke, S.L. May, Y. Shen, D.C. Nelson, Purification and Characterization of Biofilm-Associated EPS Exopolysaccharides from ESKAPE Organisms and Other Pathogens, PLoS One. 8 (2013) e67950. doi:10.1371/journal.pone.0067950.

[14] M.C. Walters, F. Roe, A. Bugnicourt, M.J. Franklin, P.S. Stewart, Contributions of antibiotic penetration, oxygen limitation, and low metabolic activity to tolerance of Pseudomonas aeruginosa biofilms to ciprofloxacin and tobramycin, Antimicrob. Agents Chemother. 47 (2003) 317–323. doi:10.1128/AAC.47.1.317-323.2003.

[15] J.N. Anderl, M.J. Franklin, P.S. Stewart, Role of Antibiotic Penetration Limitation in Klebsiella pneumoniae Biofilm Resistance to Ampicillin and Ciprofloxacin, 44 (2000) 1818–1824.

[16] R. Singh, P. Ray, A. Das, M. Sharma, Penetration of antibiotics through Staphylococcus aureus and Staphylococcus epidermidis biofilms, J. Antimicrob. Chemother. 65 (2010) 1955–1958. doi:10.1093/jac/dkq257.

[17] W.L. Jones, M.P. Sutton, L. Mckittrick, P.S. Stewart, Chemical and antimicrobial treatments change the viscoelastic properties of bacterial biofilms, Biofouling. 27 (2011) 207–215. doi:10.1080/08927014.2011.554977.

[18] N.M. Abraham, S. Lamlertthon, V.G. Fowler, K.K. Jefferson, Chelating agents exert distinct effects on biofilm formation in Staphylococcus aureus depending on strain background: Role for clumping factor B, J. Med. Microbiol. 61 (2012) 1062–1070. doi:10.1099/jmm.0.040758-0.

[19] Y. Itoh, X. Wang, B. Joseph Hinnebusch, J.F. Preston, T. Romeo, Depolymerization of β- 1,6-N-acetyl-D-glucosamine disrupts the integrity of diverse bacterial biofilms, J.Bacteriol. 187 (2005) 382–387. doi:10.1128/JB.187.1.382-387.2005.

[20] P. Chaignon, I. Sadovskaya, C. Ragunah, N. Ramasubbu, J.B. Kaplan, S. Jabbouri, Susceptibility of staphylococcal biofilms to enzymatic treatments depends on their chemical composition, Appl. Microbiol. Biotechnol. 75 (2007) 125–132. doi:10.1007/s00253-006-0790-y.

[21] C.B. Whitchurch, T. Tolker-Nielsen, P.C. Ragas, J.S. Mattick, Extracellular DNA required for bacterial biofilm formation, Science (80-. ). 295 (2002) 1487. doi:10.1126/science.295.5559.1487.

[22] N. Ramasubbu, L.M. Thomas, C. Ragunath, J.B. Kaplan, Structural analysis of dispersin B, a biofilm-releasing glycoside hydrolase from the periodontopathogen Actinobacillus actinomycetemcomitans, J. Mol. Biol. 349 (2005) 475–486. doi:10.1016/j.jmb.2005.03.082.

[23] J.B. Kaplan, C. Ragunath, K. Velliyagounder, D.H. Fine, N. Ramasubbu, Enzymatic detachment of Staphylococcus epidermidis biofilms, Antimicrob. Agents Chemother. 48 (2004) 2633–2636. doi:10.1128/AAC.48.7.2633-2636.2004.

[24] M. Jamal, W. Ahmad, S. Andleeb, F. Jalil, M. Imran, M.A. Nawaz, T. Hussain, M. Ali, M. Rafiq, M.A. Kamil, Bacterial biofilm and associated infections, J. Chinese Med. Assoc. 81 (2018) 7–11. doi:10.1016/j.jcma.2017.07.012.

[25] M.R. Parsek, P.K. Singh, Bacterial Biofilms: An Emerging Link to Disease Pathogenesis, Annu. Rev. Microbiol. 57 (2003) 677–701. doi:10.1146/annurev.micro.57.030502.090720.

[26] R.M. Donlan, Biofilms and device-associated infections, Emerg. Infect. Dis. 7 (2001) 277–281. doi:10.3201/eid0702.010226.

[27] Y. Chao, L.R. Marks, M.M. Pettigrew, A.P. Hakansson, Streptococcus pneumoniae biofilm formation and dispersion during colonization and disease, Front. Cell. Infect. Microbiol. 4 (2015) article 194. doi:10.3389/fcimb.2014.00194.

[28] G. Donelli, I. Francolini, D. Romoli, E. Guaglianone, A. Piozzi, C. Ragunath, J.B. Kaplan, Synergistic activity of dispersin B and cefamandole nafate in inhibition of staphylococcal biofilm growth on polyurethanes, Antimicrob. Agents Chemother. 51 (2007) 2733–2740. doi:10.1128/AAC.01249-06.

[29] J.H. Lee, J.B. Kaplan, W.Y. Lee, Microfluidic devices for studying growth and detachment of Staphylococcus epidermidis biofilms, Biomed. Microdevices. 10 (2008) 489–498. doi:10.1007/s10544-007-9157-0.

[30] R.O. Darouiche, M.D. Mansouri, P. V. Gawande, S. Madhyastha, Antimicrobial and antibiofilm efficacy of triclosan and DispersinB® combination, J. Antimicrob. Chemother. 64 (2009) 88–93. doi:10.1093/jac/dkp158.

[31] V. Venketaraman, A.K. Lin, A. Le, S.C. Kachlany, N.D. Connell, J.B. Kaplan, Both leukotoxin and poly-N-acetylglucosamine surface polysaccharide protect Aggregatibacter actinomycetemcomitans cells from macrophage killing, Microb. Pathog. 45 (2008) 173–180. doi:10.1016/j.micpath.2008.05.007.

[32] P.C. Sharma, A. Jain, S. Jain, Fluoroquinolone antibacterials: A review on chemistry, microbiology and therapeutic prospects, Acta Pol. Pharm. - Drug Res. 66 (2009) 587–604.

[33] C. Florindo, A. Costa, C. Matos, S.L. Nunes, A.N. Matias, C.M.M. Duarte, L.P.N. Rebelo, L.C. Branco, I.M. Marrucho, Novel organic salts based on fluoroquinolone drugs: Synthesis, bioavailability and toxicological profiles, Int. J. Pharm. 469 (2014) 179–189. doi:10.1016/j.ijpharm.2014.04.034.

[34] J.M. Domagala, Structure-activity and structure-side-effect relationships for the quinolone antibacterials, J. Antimicrob. Chemother. 33 (1994) 685–706. doi:10.1093/jac/33.4.685.

[35] E.A. Jefferson, E.E. Swayze, S.A. Osgood, A. Miyaji, L.M. Risen, L.B. Blyn, Antibacterial activity of quinolone-macrocycle conjugates, Bioorganic Med. Chem. Lett. 13 (2003) 1635–1638. doi:10.1016/S0960-894X(03)00285-3.

[36] G.M. Pacifici, G. Marchini, Review Article (Pages: 5023-5041) Effects and Pharmacokinetics, Int J Pediatr. 5 (2017) 5023–5041. doi:10.22038/ijp.2017.23193.1952.

[37] K. Matsuo, M. Azuma, M. Kasai, I. Hanji, I. Kimura, T. Kosugi, N. Suga, M. Satoh, Investigation of the clinical efficacy and dosage of intravenous ciprofloxacin in patients with respiratory infection, J. Pharm. Pharm. Sci. 11 (2008) 111s–117s. doi:10.18433/J3X30C.

[38] E. Ohki, Y. Yamagishi, H. Mikamo, Relationship between the clinical efficacy and AUC/MIC of intravenous ciprofloxacin in Japanese patients with intraabdominal infections, J. Infect. Chemother. 19 (2013) 951–955. doi:10.1007/s10156-012-0512-6.

[39] M. V. Rekharsky, Y. Inoue, Complexation Thermodynamics of Cyclodextrins, Chem. Rev. 98 (1998) 1875–1917. doi:10.1021/cr970015o.

[40] R. Villalonga, R. Cao, A. Fragoso, Supramolecular Chemistry of Cyclodextrins in Enzyme Technology, Chem. Rev. 107 (2007) 3088−3116. doi:10.1021/cr050253g.

[41] M. Fernández, A. Fragoso, R. Cao, M. Baños, R. Villalonga, Chemical conjugation of trypsin with monoamine derivatives of cyclodextrins: Catalytic and stability properties, Enzyme Microb. Technol. 31 (2002) 543–548. doi:10.1016/S0141-0229(02)00151-5.

[42] M. Fernández, M. de L. Villalonga, A. Fragoso, R. Cao, R. Villalonga, Stabilization of $\alpha$- chymotrypsin by modification with β-cyclodextrin derivatives, Biotechnol. Appl. Biochem. 36 (2002) 235–239. doi:10.1042/BA20020056.

[43] R. Villalonga, M. Fernández, A. Fragoso, R. Cao, L. Mariniello, R. Porta, Thermal stabilization of trypsin by enzymic modification with β-cyclodextrin derivatives, 2003. doi:10.1042/BA20020096.

[44] M. Fernández, A. Fragoso, R. Cao, R. Villalonga, Stabilization of $\alpha$-chymotrypsin by chemical modification with monoamine cyclodextrin, Process Biochem. 40 (2005) 2091–2094. doi:10.1016/j.procbio.2004.07.023.

[45] R. Villalonga, S. Tachibana, R. Cao, H.L. Ramirez, Y. Asano, Supramolecular-mediated thermostabilization of phenylalanine dehydrogenase modified with β-cyclodextrin derivatives, Biochem. Eng. J. 30 (2006) 26–35. doi:10.1016/j.bej.2006.01.013.

[46] A. Štimac, M. Šekutor, K. Mlinarić-Majerski, L. Frkanec, R. Frkanec, Adamantane in drug delivery systems and surface recognition, Molecules. 22 (2017) 297. doi:10.3390/molecules22020297.

[47] M.E. Brewster, T. Loftsson, Cyclodextrins as pharmaceutical solubilizers, Adv. Drug Deliv. Rev. 59 (2007) 645–666. doi:10.1016/j.addr.2007.05.012.

[48] R.L. Carrier, L.A. Miller, I. Ahmed, The utility of cyclodextrins for enhancing oral bioavailability, J. Control. Release. 123 (2007) 78–99. doi:10.1016/j.jconrel.2007.07.018.

[49] K.C. Nicolaou, T. Lister, R.M. Denton, A. Montero, D.J. Edmonds, Adamantaplatensimycin: A bioactive analogue of platensimycin, Angew. Chemie - Int. Ed. 46 (2007) 4712–4714. doi:10.1002/anie.200701548.

[50] H.-J. Schneider, F. Hacket, V. Rüdiger, H. Ikeda, NMR Studies of Cyclodextrins and Cyclodextrin Complexes, Chem. Rev. 98 (1998) 1755–1785. doi:10.1021/cr970019t.

[51] R. Krishnan, A.M. Rakhi, K.R. Gopidas, Study of β-cyclodextrin-pyromellitic diimide complexation. Conformational analysis of binary and ternary complex structures by induced circular dichroism and 2D NMR spectroscopies, J. Phys. Chem. C. 116 (2012) 25004–25014. doi:10.1021/jp309788z.

[52] M.W. Freyer, E.A. Lewis, Isothermal Titration Calorimetry: Experimental Design, Data Analysis, and Probing Macromolecule/Ligand Binding and Kinetic Interactions, Methods Cell Biol. 84 (2008) 79–113. doi:10.1016/S0091-679X(07)84004-0.

[53] T. Wiseman, S. Williston, J.F. Brandts, N. Lint, Rapid Measurement of Binding Constants and Heats of Binding Using a New Titration Calorimeter, Anal. Biochem. 179 (1989) 131–137.

[54] A. Velazquez-Campoy, Geometric features of the Wiseman isotherm in isothermal titration calorimetry, J. Therm. Anal. Calorim. 122 (2015) 1477–1483. doi:10.1007/s10973-015-4775-x.

[55] W.B. Turnbull, A.H. Daranas, On the Value of c: Can Low Affinity Systems Be Studied by Isothermal Titration Calorimetry?, J. Am. Chem. Soc. 125 (2003) 14859–14866. doi:10.1021/ja036166s.

[56] D.L. Cameron, J. Jakus, S.R. Pauleta, G.W. Pettigrew, A. Cooper, Pressure perturbation calorimetry and the thermodynamics of noncovalent interactions in water: Comparison of protein-protein, protein-ligand, and cyclodextrin-adamantane complexes, J. Phys. Chem. B. 114 (2010) 16228–16235. doi:10.1021/jp107110t.

[57] J. Carrazana, A. Jover, F. Meijide, V.H. Soto, J.V. Tato, Complexation of adamantly compounds by β-cyclodextrin and monoaminoderivatives, J. Phys. Chem. B. 109 (2005) 9719–9726. doi:10.1021/jp0505781.

[58] L. Liu, Q.X. Guo, The driving forces in the inclusion complexation of cyclodextrins, J. Incl. Phenom. 42 (2002) 1–14. doi:10.1023/A:1014520830813.

[59] P.D. Ross, M. V. Rekharsky, Thermodynamics of hydrogen bond and hydrophobic interactions in cyclodextrin complexes, Biophys. J. 71 (1996) 2144–2154. doi:10.1016/S0006-3495(96)79415-8.

[60] T. Higuchi, K.A. Connors, Phase Solubility Techniques, in: Reilly C.N. (Ed.), Adv. Anal. Chem. Instrum., Interscience, New York, NY, 1965: pp. 117–212.

[61] T. Loftsson, D. Hreinsdóttir, M. Másson, Evaluation of cyclodextrin solubilization of drugs, Int. J. Pharm. 302 (2005) 18–28. doi:10.1016/j.ijpharm.2005.05.042.

[62] European Committee for Antimicrobial Susceptibility Testing (EUCAST) of the European Society of Clinical Microbiology and Infectious Diseases (ESCMID), Determination of minimum inhibitory concentrations (MICs) of antibacterial agents by broth dilution, Clin.Microbiol.Infect. 9 (2003) 1–7. doi:10.1046/j.1469-0691.2003.00790.x.

[63] Y. Nait Chabane, M. Ben Mlouka, S. Alexandre, M. Nicol, S. Marti, M. Pestel-Caron, J.Vila, T. Jouenne, E. Dé, Virstatin inhibits biofilm formation and motility of Acinetobacter baumannii, BMC Microbiol. 14 (2014) 62. doi:10.1186/1471-2180-14-62.

[64] D. Mack, W. Fischer, A. Krokotsch, K. Leopold, R. Hartmann, H. Egge, R. Laufs, The intercellular adhesin involved in biofilm accumulation of Staphylococcus epidermidis is a linear β-1,6-linked glucosaminoglycan: Purification and structural analysis, J. Bacteriol. 178 (1996) 175–183. doi:10.1128/jb.178.1.175-183.1996.

[65] I. Sadovskaya, E. Vinogradov, S. Flahaut, G. Kogan, S. Jabbouri, Extracellular carbohydrate-containing polymers of a model biofilm-produring strain, Staphylococcus epidermidis RP62A, Infect. Immun. 73 (2005) 3007–3017. doi:10.1128/IAI.73.5.3007-3017.2005.

[66] G. Kogan, I. Sadovskaya, P. Chaignon, A. Chokr, S. Jabbouri, Biofilms of clinical strains of Staphylococcus that do not contain polysaccharide intercellular adhesin, FEMS Microbiol. Lett. 255 (2006) 11–16. doi:10.1111/j.1574-6968.2005.00043.x.

[67] V.J. Stella, V.M. Rao, E.A. Zannou, V. Zia, Mechanisms of drug release from cyclodextrin complexes, Adv. Drug Deliv. Rev. 36 (1999) 3–16. doi:10.1016/S0169-409X(98)00052-0.

[68] V.J. Stella, R.A. Rajewski, Cyclodextrins: Their Future in Drug Formulation and Delivery, Pharm. Res. 14 (1997) 556–567.

[69] T. Loftsson, M.D. Moya-Ortega, C. Alvarez-Lorenzo, A. Concheiro, Pharmacokinetics of cyclodextrins and drugs after oral and parenteral administration of drug/cyclodextrin complexes, J. Pharm. Pharmacol. 68 (2016) 544–555. doi:10.1111/jphp.12427.

[70] T. Carofiglio, M. Cordioli, R. Fornasier, L. Jicsinszky, U. Tonellato, Synthesis of 6Iamino-6I-deoxy-2I-VII, 3I-VII-tetradeca-O-methyl-cyclomaltoheptaose, Carbohydr. Res. 339 (2004) 1361–1366. doi:10.1016/j.carres.2004.03.007.

[71] A. Angelova, C. Fajolles, C. Hocquelet, F. Djedaïni-Pilard, S. Lesieur, V. Bonnet, B. Perly, G. Lebas, L. Mauclaire, Physico-chemical investigation of asymmetrical peptidolipidylcyclodextrins, J. Colloid Interface Sci. 322 (2008) 304–314. doi:10.1016/j.jcis.2008.03.023.

[72] G.A. O'Toole, R. Kolter, Flagellar and twitching motility are necessary for Pseudomonas aeruginosa biofilm development, Mol. Microbiol. 30 (1998) 295–304. doi:10.1046/j.1365-2958.1998.01062.x.

[73] F. Costa, I.F. Carvalho, R.C. Montelaro, P. Gomes, M.C.L. Martins, Covalent immobilization of antimicrobial peptides (AMPs) onto biomaterial surfaces, Acta Biomater. 7 (2011) 1431–1440. doi:10.1016/j.actbio.2010.11.005.

[74] D. Campoccia, L. Montanaro, C.R. Arciola, A review of the biomaterials technologies for infection-resistant surfaces, Biomaterials. 34 (2013) 8533–8554. doi:10.1016/j.biomaterials.2013.07.089.

[75] K. Glinel, P. Thebault, V. Humblot, C.M. Pradier, T. Jouenne, Antibacterial surfaces developed from bio-inspired approaches, Acta Biomater. 8 (2012) 1670–1684. doi:10.1016/j.actbio.2012.01.011.

[76] P.L. Shah, S.F. Scott, R.A. Knight, C. Marriott, C. Ranasinha, M.E. Hodson, In vivo effects of recombinant human DNase I on sputum in patients with cystic fibrosis, Thorax. 51 (1996) 119–125. doi:10.1136/thx.51.2.119.

[77] J.N. Zitter, P. Maldjian, M. Brimacombe, K.P. Fennelly, Inhaled Dornase alfa (Pulmozyme) as a noninvasive treatment of atelectasis in mechanically ventilated patients, J. Crit. Care. 28 (2013) 218.e1–218.e7. doi:10.1016/j.jcrc.2012.09.015.